Design of an efficient monochromatic electron source for inverse photoemission spectroscopy*

GENG Dong-Ping(耿东平)[1,2] YANG Ying-Guo(杨迎国)[1] LIU Shu-Hu(刘树虎)[2]
HONG Cai-Hao(洪才浩)[2;1)] GAO Xing-Yu(高兴宇)[1;2)]

[1] Shanghai Institute of Applied Physics, Chinese Academy of Sciences, Shanghai 201800, China
[2] Institute of High Energy Physics, Chinese Academy of Sciences, Beijing 100049, China

Abstract: A design for an efficient monochromatic electron source for Inverse Photoemission Spectroscopy (IPES) apparatus is described. The electron source consists of a BaO cathode, a focus electrostatic lens, a hemispherical deflection monochromator (HDM), and a transfer electrostatic lens. The HDM adopts a "slit-in and slit-out" structure and the degradation of first-order focusing is corrected by two electrodes between the two hemispheres, which has been investigated by both analytical methods and electron-ray tracing simulations using the SIMION program. Through the focus lens, the HDM, and the standard five-element transfer lens, an optimal energy resolution is estimated to be about 53 MeV with a beam flux of 27 μA. Pass energy (P.E.) of 10 eV and 5 eV are discussed, respectively.

Key words: beam flux, electrostatic lens, hemispherical deflection monochromator, fringing effect, energy resolution, SIMION

PACS: 41.85.Ne, 41.85Qg, 41.85.Ja **DOI:** 10.1088/1674-1137/38/11/118202

1 Introduction

Although photoemission spectroscopy provides a powerful tool for the characterization of occupied electronic states, it cannot detect those which are unoccupied. These unoccupied states can be probed by two-photo photoemission (2PPE) or inverse photoemission spectroscopy (IPES); however, 2PPE covers only a small part of a typical Brillouin zone in spite of its high energy resolution [1]. IPES, on the other hand, can cover the dispersion of unoccupied states with sufficient accuracy in a wider energy range above the Fermi level. In IPES, an incident electron is ejected into an unoccupied state and creates a radiative transition to another unoccupied state above the Fermi level, working in an inverse mode compared with PES. The photon emitted in this transition needs to be detected. Consequently, an electron source and a photon detector are essential in the IPES measurements. As the inverse photoemission process has rather low cross sections, the photon detectors in IPES suffer from quite low counting rates [2]. Therefore, a special effort should be dedicated to increase the intensity of the electron sources to make up for the low counting rates of the outgoing photons [3]. To achieve high emission rates, the cathode of the electron sources is often made of material with a low work function. However, the space charge effects become very severe for the low kinetic energy electrons used in IPES, which prevents the beam intensity becoming too high. On the other hand, as an important parameter determining the performance of the IPES apparatus, the energy resolution is determined by two factors: the energy spread of the electron source and the bandpass of the photon detector. Geiger-Müller-based photon detectors with a relatively narrow bandpass can be achieved with various combinations of entrance windows and filled gases [4–6]. Thus, the energy spread of the electron source often becomes the key factor in determining the overall energy resolution of the IPES apparatus [7].

In this article, we describe a design for a high-efficiency monochromatic electron source for IPES. The whole system was analyzed and simulated using an electron-ray tracing simulation program, SIMION. To overcome the space charge limitation at the low electron kinetic energy (KE) range, electrons in the present design are first generated at higher energy and later decelerated to the low KE used. In addition, a slit structure is used rather than an aperture, due to its larger acceptance,

Received 15 January 2014, Revised 5 May 2014

∗ Supported by National Natural Science Foundation of China (11175239), One Hundred Person Project of Chinese Academy of Sciences, and Instrument design and development Project of CAS: Spin rosolved Inverse-PES system

1) E-mail: hongch@ihep.ac.cn

2) E-mail: gaoxy@sinap.ac.cn

which allows higher beam intensity. To reduce the energy spread of the electron source, a hemispherical deflection monochromator (HDM) was adopted.

2 Design of the electron gun

The first unit of the electron source in this design consists of a cathode and a focus electrostatic lens, which forms an electron gun (as used in most applications). To improve the efficiency of the electron source, a cathode with high emission efficiency is necessary. For thermal emission, a BaO cathode is usually used because of its low cost, low energy spread due to its low working temperature, and high emission efficiency due to its low work function. The BaO cathode works at a temperature of about 1100 K. The energy distribution of thermally emitted electrons from the BaO cathode has its maximum at $E_{\max}=kT$ with a half-width of about $2.45kT$ (k represents the Boltzmann constant) [8]. Therefore, the natural energy spread of the BaO cathode can be calculated to be about 232.5 MeV. The energy spread of the electron beam will stay constant after passing through an electrostatic lens due to the fact that all electrons are accelerated or decelerated together. Note that the initial electron velocity is not zero and the emitted electrons have an energy spread. In the following analysis and simulation, we assume an initial electron KE of 0.4 eV.

Several designs of electron gun for IPES can be found in the literature [3, 9–11]; however, there is much to be done to fully meet the demands of both intense emission and the narrow energy spread desired for IPES. The brightness of the Pierce diode gun [9] at quite low energies is limited by space charge effects because of the relatively low electric fields at the cathode surface. The low-voltage and high-current electron gun designed by Erdman and Zipf does not suit the electron KE of nearly 10 eV [10]. Since electrons from a BaO cathode are emitted in a wide range of directions, lens systems are always used to focus as many electrons as possible in the desired direction in more sophisticated IPES electron guns. In a practical lens system, the number of parameters one wants to control independently determines the complexity of the lens system. Generally, the following requirements are often needed for a lens system: (a) fixed object and image positions; (b) control of beam angle; (c) fixed linear or angular magnification; and, (d) alterable electron energy at the exit side for electrons of fixed energy at the entrance side. Usually, a minimum of two cylinder lens elements are necessary to fulfill any one of the above requirements, with one extra element added to fulfill one more requirement [12]. In the present design for IPES, the object and the image positions need to be fixed with the linear magnification constant to control the electron beam angle at the exit side, which means that requirements (a), (b), and (c) need to be fulfilled. An electrostatic lens with four cylinder elements is therefore needed. In this articles, a gun design similar to that used by Stoffel and Johnson [3] is adopted, as shown in Fig. 1. The BaO cathode, element 1 and element 2 as a whole are called an immersion objective lens, which mainly prefocuses the electron beam. According to Child's law, the space charge limited current density is [13]

$$J=\frac{4\varepsilon_0}{9}\sqrt{2\frac{e}{m}}\left(\frac{V^{3/2}}{d^2}\right), \tag{1}$$

where V is the anode-cathode potential difference, d is the distance between the anode and the cathode, e is the negative electric charge carried by a single electron, m is the mass of a single electron, and ε_0 is the permittivity of vacuum.

From Eq. (1), increasing $V_{1\mathrm{f}}$ in Fig. 1 will reduce the space charge effect, with more electrons attracted from the cathode. In Fig. 1, $V_{4\mathrm{f}}$ determines the electron KE at the exit side and $V_{3\mathrm{f}}$ is the key parameter to focus the electron beam.

The simulation results using the SIMION program are shown in Fig. 2. The electron gun can be operated with electron pass energies (P.E.) of 5 eV and 10 eV at the exit side. The characteristic lens diameters D1 and D2 are 8 mm and 12.5 mm, respectively. All the dimensional parameters of the lens are listed in Table 1. The lens tables (P.E. of 10 eV and 5 eV) are given in Table 2, respectively.

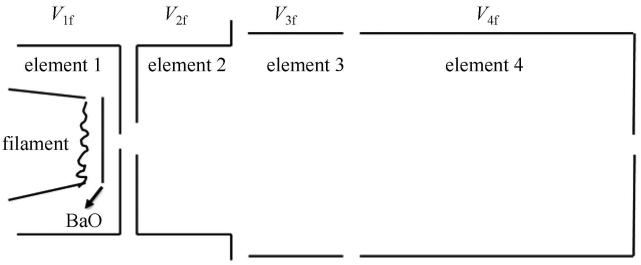

Fig. 1. A schematic diagram of the electron gun. $V_{1\mathrm{f}}$, $V_{2\mathrm{f}}$, $V_{3\mathrm{f}}$ and $V_{4\mathrm{f}}$ represent the voltages applied on element 1, 2, 3 and 4. Note that all the voltages applied are relative to ground.

Table 1. The parameters of the four-element lens.

parameter	A	G	$L_{2\mathrm{f}}$	$L_{3\mathrm{f}}$	$L_{4\mathrm{f}}$
length/mm	6.25	1.25	12	5	18.75

Table 2. Lens table for P.E. of 10 eV and 5 eV.

	BaO	$V_{1\mathrm{f}}$	$V_{2\mathrm{f}}$	$V_{3\mathrm{f}}$	$V_{4\mathrm{f}}$
P.E.=10 eV	−10	−6	200	500	0
P.E.=5 eV	−10	−6	200	180	−5

As Fig. 3 shows, the Helmholtz-Lagrange Law [12] relates to the linear magnification M_{L} and the angular magnification M_{A} of rays through an electrostatic lens to $E_{\mathrm{o}}/E_{\mathrm{i}}$, which can be expressed in the following equation:

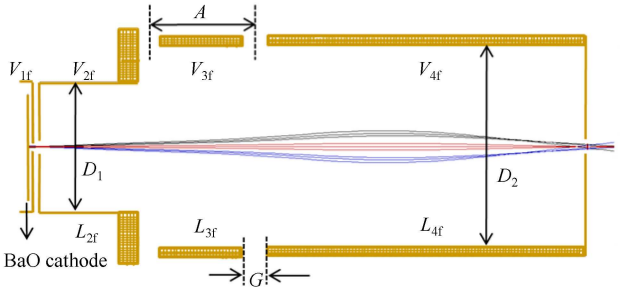

Fig. 2. Four cylinder element simulation using the SIMION program with a P.E. of 10 eV. The upper V and lower L denote the voltage applied and the length of each element, respectively.

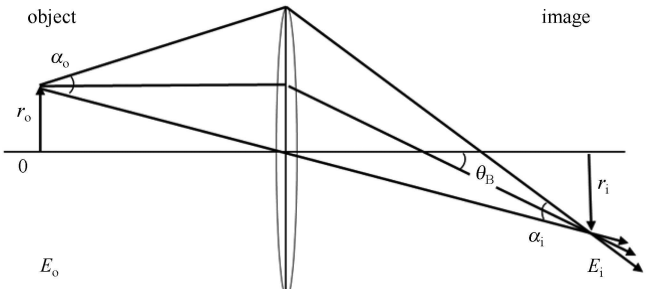

Fig. 3. Schematic drawing illustrating the Helmholtz-Lagrange Law: E_o and E_i are the electron KE at the object and image position, respectively. The linear magnification is $M_L = r_i/r_o$, where r_o and r_i represent the displacements of the object and image, respectively. Angular magnification $M_A = \alpha_i/\alpha_o$, where α_o and α_i are the pencil angles at the object and image positions, respectively. Note that the pencil angle is the half of the beam angle θ_B.

$$\left(\frac{E_o}{E_i}\right)^{\frac{1}{2}} = M_L M_A. \quad (2)$$

The beam angle θ_B (or the pencil angle α_i) is a vital parameter to later improve the energy resolution of the HDM and thus to improve the energy spread of the whole electron source. In the present design, the object position is located at the BaO cathode, with the image position at element 4 of the focus electrostatic lens. It can be seen that E_o=0.4 eV, E_i=10 eV for P. E. of 10 eV, or E_i=5 eV for P. E. of 5 eV, respectively. α_o is estimated to be about 90° based on the aperture structure of the immersion objective lens. r_0 is designed to be 0.15 mm, with $r_i \sim 1$ mm for P.E. of 10 eV and $r_i \sim 1.1$ mm for P.E. of 5 eV. The calculated values of α_i are compared with those obtained from the SIMION simulation in Table 3. According to Table 3, the calculated α_i at the exit agrees well with the SIMION simulation results.

Table 3. The calculated α_i and the SIMION simulation result α_i.

KE	α_i(calculated)	α_i(SIMION)
10 eV	2.7°	2.94°
5 eV	3.47°	3.4°

Based on the above design, an electron gun was built and its beam currents were measured as functions of V_{2f} for P.E. of 5 eV and 10 eV, as shown in Fig. 4. From Fig. 4, it can be seen that $I_{2f} = I_{1f} - I_{2f'}$ and I_{2f} reaches 200 μA when V_{2f}=200 V, where I_{1f}, $I_{2f'}$, and I_{2f} represent the current passing element 1, the current flowing through element 2, and the current passing element 2, respectively. After V_{2f} reaches 200 V, I_{2f} does not increase much with increasing V_{2f}. Note that with a P.E. of 10 eV, the beam current flux is higher than that with

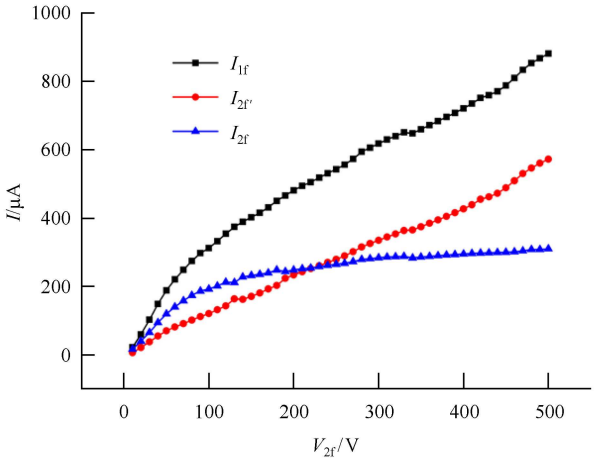

Fig. 4. Beam currents measured as functions of V_{2f}, where V_{1f}=−6 V, V_{2f}=200 V with a negative cathode bias voltage of 10 V. I_{1f} represents the current passing element 1; $I_{2f'}$: the current flowing through element 2; I_{2f}: the current passing element 2.

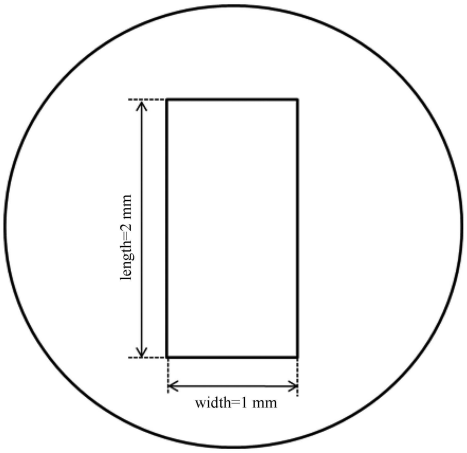

Fig. 5. The slit behind element 4.

P.E. of 5 eV because the higher anode voltage will extract more electrons from the cathode. In the experimental setup there is a slit (as shown in Fig. 5) at the exit of element 4 to allow only a part of the electrons through. Considering an electron beam image with a diameter of about 1 mm at the exit of element 4, about 64% of the beam current can pass through this slit, which means that a beam flux of nearly 128 μA can be obtained with V_{2f}=200 V.

3 Design of the hemispherical deflection monochromator

3.1 Principles of the hemispherical deflection monochromator

As discussed above, the energy spread of the electron beam out of the focus lens in the present setup remains about 232.5 MeV. To reduce the energy distribution width, an HDM is adopted. As shown in Fig. 6, if E_0 is the P.E. of electrons traveling along the orbit with a radius R_0=(R_1+R_2)/2, then the voltages on the inner and outer hemispheres, V_1 and V_2, are given by

$$V_{1,2}=V_0\left(\frac{2R_0}{R_{1,2}}-1\right). \tag{3}$$

With R_1=50 mm and R_2=70 mm, it can be obtained that V_1=7 V and V_2=3.5714 V for P.E.=5 eV, whereas V_1=14 V and V_2=7.1429 V for P.E.=10 eV. The energy resolution or full width at half maximum (FWHM) of the electron with P.E. passing through the HDM can be given by [14]

$$\frac{\Delta E_{(\mathrm{FWHM})}}{\mathrm{P.E.}}\approx\frac{0.86\omega}{2R_0}+0.25\theta_{\mathrm{B}}^2. \tag{4}$$

In Eq. (4), ω and θ_{B} stand for the entrance slit width and the angle of the emitted electron beam divergence from the HDM, as shown in Fig. 6. The formula given above works when $\omega/R_0\leqslant0.1$, $\alpha_{\max}/\alpha_0\leqslant2$, and $\alpha_{\max}<0.24$, where $\alpha_0=(\omega/4R_0)^{1/2}$.

The entrance and exit slit width ω is 1 mm and the incidence beam angle is expected to be 5.9° for 10 eV and 6.8° for 5 eV, respectively, which is decided by the focus electrostatic lens discussed in section 2. Accordingly, the energy resolution is about 53 MeV for P.E.=5 eV and 98 MeV for P.E.=10 eV, respectively. Because the energy spread of the electrons emitted from BaO cathode is 232.5 MeV, the transmission of the HDA can be estimated to be about 0.212 for P.E.=10 eV and 0.381 for P.E.=10 eV. Thus, an electron beam flux can reach 27 μA for P.E.=5 eV and 49 μA for P.E.=10 eV after the exit slit of the HDA. It can be seen that for a P.E. of 5 eV, a higher energy resolution (a smaller energy spread) can be achieved but with a lower electron beam flux. Therefore, a compromise must be made between the beam flux and the energy resolution. In most cases, an aperture structure is often adopted at both the entrance and exit of an HDM due to its simplicity. However, they are not suitable for achieving high beam flux because many electrons are blocked. One of its main advantages over Cylindrical Mirror Analyzers and other dispersion-type energy monochromators is that a HDM can realize two-dimensional focusing to achieve high transmission with the same energy resolution. To realize such an advantage, the rectangular slit structure shown in Fig. 5 was adopted at both entrance and exit, with the one at the entrance serving as the exit slit of the electron gun, which was described previously. The overall setup is thus called a "slit-in and slit-out" structure. Given the aperture diameter and the slit width to be 1 mm, the area of the slit in Fig. 5 can be calculated to be 2 mm^2 and that of the aperture is 0.8 mm^2. Obviously, a slit structure with a larger area is more efficient for transmitting electrons than an aperture one structure [15]. From Equation 4, ω is a key factor determining energy resolution in an HDM and a larger ω means a worse energy resolution. By using a larger aperture diameter to get higher electron transmission for the aperture structure, enlarging the electron energy width is inevitable. However, this problem can be solved when the slit structure shown in Fig. 5 is adopted. The length can be increased with more electrons transmitted, but with the width kept constant and without the energy width being increased.

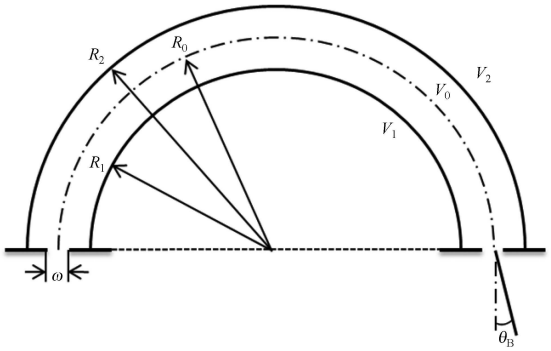

Fig. 6. A hemispherical deflection monochromator.

3.2 Correction of the fringing effect

In practice, an HDM has fringing fields at both entrance and exit slits, which means that strong leakage fields inside and outside the hemispheres lead to field distortions, as shown in Fig. 7(a). These fields will obviously hinder the performance of the HDM. Intense efforts have been dedicated to eliminate the fringing field effects, and various correction schemes have been employed, such as Herzog plates, Jost electrodes, tilted input beam axis, and multiple rings or strips [16]. However, each of these schemes have their own shortcomings, such as low effectiveness, complex fabrication, and difficult optimization [17].

The simulation results of an HDM using the SIMION program are shown in Fig. 7. In Fig. 7(a), electric field distortions are present at both the entrance and exit slits. Owing to the distortions, the degradation of the first-order focusing is shown in Fig. 7(b), in which the focal point (the red cross) is not located at the exit slit and the beam axis is shifted sidewards. This can lead to transmission losses and a worse energy resolution. Here, a delicate and simple solution is adopted, with two more electrodes added inside the space between the two hemispheres near both the entrance and exit, respectively, as shown in Fig. 8. By tuning the voltages of the two electrodes, the degradation of the first-order focusing can be corrected perfectly. From Fig. 8, it can be seen that the electron beam focuses perfectly at the exit slit without the beam axis angle being shifted. The voltages applied on the five electrodes in Fig. 8, which are optimized from SIMION program simulations, are listed in Table 4 for P.E. of 10 eV and 5 eV, respectively.

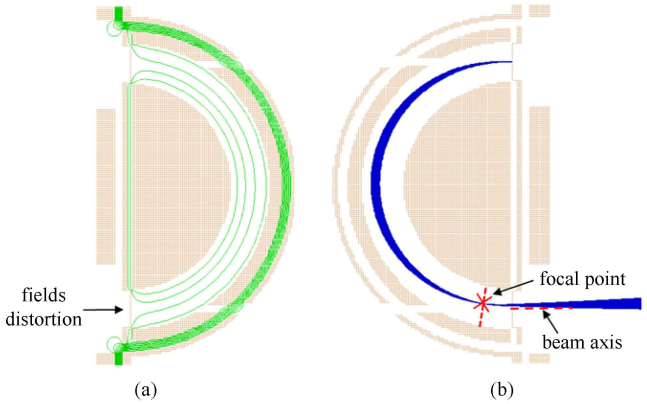

Fig. 7. (color online) (a) The SIMION simulation of an HDM when P.E.=10 eV. The green lines denote the equipotential lines. (b) Degradation of first-order focusing of an HDM when P.E.=10 eV.

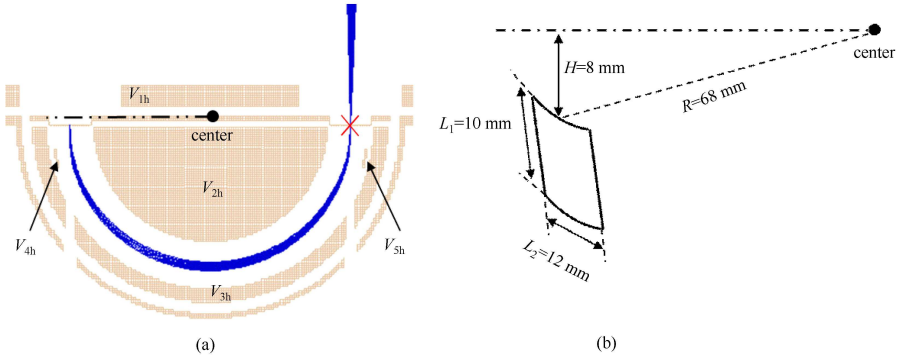

Fig. 8. (a) The HDM correction scheme with two electrodes added symmetrically at both sides (P.E.=10 eV). (b) Detailed layout of the electrode structure at the entrance with its position between the hemispheres. The electrode is a part cut from a sphere (concentric with the two hemispheres), with a thickness of 0.1 mm and a radius R of 68 mm.

Table 4. The voltages of the five electrodes for P.E. 10 eV and 5 eV.

	V_{1h}	V_{2h}	V_{3h}	V_{4h}	V_{5h}
P.E.=10 eV	0	4	−2.73	−3.5	−3.5
P.E.=5 eV	−5	−3.055	−6.4	−6.75	−6.6

4 Design of the transfer electrostatic lens

The ability to tune KE is essential for IPES. The electrons out of the HDM need to be accelerated or decelerated to tune their KE to probe different electronic structures at different energy levels above the Fermi level of the materials. Therefore, a transfer electrostatic lens has to be mounted after the exit slit of the HDM, which allows the electrons (at the constant 5 eV or 10 eV KE) to be tuned continuously from 5 eV to 20 eV (the general scan KE range in IPES). To achieve high efficiency in IPES, the electrons of variable KE should be focused well on the samples after this lens.

Here, a standard five-element zoom lens is selected. A schematic view of this lens with its parameters is shown in Fig. 9. The distance unit used in this lens, or its characteristic value, is the cylinder diameter D=20 mm. Here, A/D=0.5 and G/D=0.1. The other distances of the lens are given in Table 5. The KE of ejected electrons from this lens is determined by the difference between V_{5t} and V_{1t}. In this design, $V_{3t}/V_{1t} = V_{5t}/V_{3t}$. V_{2t} and V_{4t} of the middle electrodes can be tuned to keep the image position (i.e. the sample position) constant [18]. It should be noted that the HDM supporting plate (V_{1h}), element 4 of the focus lens (V_{4f}), and the first element of transfer lens (V_{1t}) are in electrical contact. Therefore, $V_{1t} = V_{1h} = V_{4f}$. In the five-element transfer lens in this paper, the KE of incoming electrons is denoted as KE_0 and that of outgoing electrons as KE_1. With the known KE_0, KE_1, and V_{1t}, the V_{5t} applied can be calculated as

follows: V_{5t}=KE$_1$/e-KE$_0$/e+V_{1t}. The features of the standard five-element zoom lens (A/D=0.5) have been thoroughly studied to understand the relations of working distance and voltages of each element [18–21]. However, in practice, the lens needs to be constructed to find the optimal conditions in future experiments.

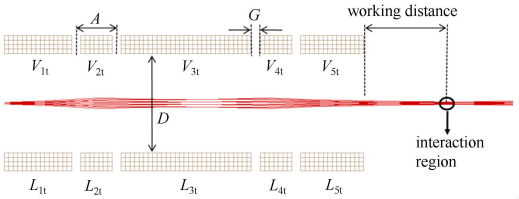

Fig. 9. The five-element transfer lens with its parameters: the upper V and lower L denote the voltage applied and the length of each element, respectively (P.E.=10 eV).

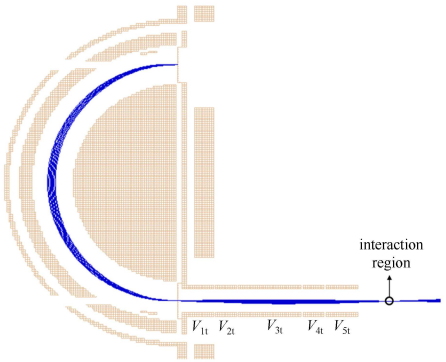

Fig. 10. The electron-ray tracing simulations of the HDM with fringing field correction and the transfer lens (P.E.=10 eV).

Finally, electron-ray tracing simulations of the present HDM using the SIMION program, with fringing field correction and the five-element transfer lens as a whole, are shown in Fig. 10. It is shown that the electron beam through the HDM and the transfer lens can be well focused on the sample. Due to the fact that there is no energy spread and beam flux loss in the five-element transfer lens, the energy resolution and beam flux are estimated to be 98 meV and 49 μA for P.E.=10 eV, and 53 meV and 27 μA for P.E.=5 eV, respectively.

Table 5. The lengths of the five-element zoom lens.

element	L_{1t}	L_{2t}	L_{3t}	L_{4t}	L_{5t}
length/mm	25	10	50	10	25

5 Conclusion

In this paper, an efficient monochromatic electron source for IPES has been designed in detail. The initial test shows that the beam flux can reach 128 μA at the exit slit of the focus electrostatic lens. A specially designed HDM is adopted after the focus electrostatic lens to reduce the energy spread of the electron beam. Adding two extra electrodes between the hemispheres perfectly solves the degradation of the first-order focusing after the HDM. The energy spread of the electron beam after the HDM is calculated to be 98 MeV and 53 MeV for 10 eV and 5 eV P.E., respectively. A "slit-in and slit-out" structure is adopted in favor of a high beam flux with a good energy resolution. A standard five-element zoom lens is then adopted after the HDM to tune the KE of the electrons emitted. The beam flux of the whole setup is estimated to be 49 μA for P.E.=10 eV, and 27 μA for P.E.=5 eV with an energy spread of 98 MeV and 53 MeV, respectively. The whole design makes it possible for the electron source to achieve high beam flux with narrow energy spread, which is ideal for IPES to study electronic states with high energy resolution.

References

1 Stiepel R, Ostendorf R, Benesch C et al. Rev. Sci. Instrum., 2005, **76**(6): 063109
2 Budke M, Renken V, Liebl H et al. Rev. Sci. Instrum., 2007, **78**(8): 083903
3 Stoffel N G, Johnson P D. Nucl. Instrum. Methods Phys. Res. A, 1985, **234**(2): 230–234
4 Maniraj M, D'Souza S W, Nayak J et al. Rev. Sci. Instrum., 2011, **82**(9): 093901
5 Funnemann D, Merz H. J. Phys. E: Sci. Instrum., 1986, **19**: 554
6 Nakatake M, Okamura Y, Akiyama S et al. J. Electron. Spectrosc. Relat. Phenom, 1998, **88**: 1027–1030
7 Johnson P D, Hulbert S L. Rev. Sci. Instrum., 1990, **61**(9): 2277
8 Young R D. Phys. Rev., 1959, **113**(1): 110
9 Pierce J R. J. Appl. Phys., 1940, **11**(8): 548–554
10 Erdman P W, Zipf E C. Rev. Sci. Instrum., 1982, **53**(2): 225
11 Simpson J A, Kuyatt C E. Rev. Sci. Instrum., 1963, **34**(3): 265
12 Granneman E H A, Van der Wiel M J. In: Handbook on Synchrotron Radiation, Vol. 1. eds. Koch E E, Sasaki T, Winick H. Amsterdam: North-Holland, 1979. 389
13 Jensen K L, Lebowitz J, Lau Y Y et al. J. Appl. Phys., 2012, **111**(5): 054917
14 Imhof R E, Adams A, King G C. J. Phys. E, 1976, **9**(2): 138
15 LU Jia-He et al. Technology of Surface Analysis. Beijing: Publishing House of Electronics Industry, 1987. 149–151 (in Chinese)
16 Sise O, Zouros T J M, Ulu M et al. Meas. Sci. Technol., 2007, **18**(7): 1853
17 Hu D Q, Leung K T. Rev. Sci. Instrum., 1995, **66**(4): 2865
18 Dogan M, Sise O, Ulu M. Radiat. Phys. Chem., 2007, **76**(3): 445-449
19 Sise O, Ulu M, Dogan M. Nucl. Instrum. Methods Phys. Res. A, 2005, **554**(1): 114–131
20 Sise O, Ulu M, Dogan M. Radiat. Phys. Chem., 2007, **76**(3): 593–598
21 Heddle D W O, Papadovassilakis N. J. Phys. E: Sci. Instrum., 1984, **17**(7): 599